

Numerical Analysis on Reflected Shock Wave-Boundary Layer Interaction in Reactive Mixture

Mkoto Asahara*, Tsubasa Koyama*, A. Koichi Hayashi*, Nobuyuki Tsuboi**

*Department of Mechanical Engineering, Aoyama Gakuin University
5-10-1 Fuchinobe, Chuo, Sagami-hara, Kanagawa 252-5258, Japan

**Department of Machine Intelligence, Kyusyu institute of technology,
1-1 Sensui, Tobata, Kitakyusyu 804-8550, Japan

1 Introduction

Ignition delay time is obtained by measuring a time from when a shock wave reflects from tube end filled with a reactive mixture until when an ignition occurs behind reflected shock wave. Measuring ignition delay time is useful to study reaction processes and to develop chemical reaction mechanism because it can be performed under constant pressure and temperature. This technique is one-dimensional phenomena under ideal conditions. Gilbert and Strehlow^[1] showed a numerical analysis of H₂-O₂-Ar detonation originating from a reflected shock wave at the tube end. However the real phenomena have an influence by the multi-dimensional flows at the side wall boundary layer and temperature boundary layer at the side and endwalls on chemical reactions^[2]. Meanwhile Saytzev and Soloukhin^[3], Voevodsky and Soloukhin^[4], Soloukhin^[5] reported the existence of two types of ignition, sharp ignition and strong ignition, depending on incident shock wave conditions. Meyer and Oppenheim^[6] presented the experimental results using a high speed laser schlieren technique to show two types of H₂-O₂ ignition; strong ignition which is a sudden ignition at the whole cross section near the reflected wall and mild ignition which is an ignition by slowly building-up flame kernels at the area a little away from the reflected wall. They showed the ignition map at the pressure of 23~196 kPa and temperature of 900~1350 K.

Takano^[7] performed two-dimensional numerical analyses at the strong ignition conditions reported by Gilbert and Strehlow^[1] and strong and mild ignition conditions reported by Meyer and Oppenheim^[6] to show each phenomenon qualitatively. However his results may not show the real phenomena enough because the bifurcating points of reflected shock wave are quite away from the side wall comparing with experiments and because the calculated flow field is not disturbed comparing with the one in the Schlieren photos taken by Meyer and Oppenheim^[6]. Author's group calculated aluminum dust ignition induced by reflected shock wave and described the ignition mechanism by reflected shock wave^[8]. However, this result is not enough to understand about the ignition behind reflected shock wave.

Recently, Yamashita et al.^[9] conducted an experimental study of C₂H₂-O₂ detonation ignition process behind reflected shock wave to show in detail an occurrence location of flame kernels at mild ignition, which information is few in the past. They also performed numerical analysis of multi-dimensional flow by an interaction between sidewall boundary layer and reflected shock wave to try to

show a relation between the bifurcating location of reflected shock wave and occurrence location of flame kernel. However their numerical analysis did not show ignition. The recent numerical study on deflagration-to-detonation transition (DDT) showed a transition to detonation which process is similar to mild ignition in shock tube. One of DDT processes is that a precursor shock wave produces boundary layer behind it and compression waves produced by flame front interact with the boundary layer to give an auto-ignition in the boundary layer.

This study will present numerical results of auto-ignition behind a reflected shock wave in a shock tube with a reactive mixture. Two-dimensional analyses will provide reproduction of strong and mild ignition which were shown by Meyer and Oppenheim^[6].

2 Numerical methods and conditions

The governing equations are two-dimensional compressible Navier-Stokes equations with species equations which deal with H_2/O_2 chemical reaction mechanism consisting of nine species (H_2 , O_2 , O , H , OH , HO_2 , H_2O_2 , H_2O , and N_2). The NS equations use time splitting for convective terms, viscous term, production terms and discretization for each term independently. AUSMDV scheme is applied to convective terms and third-order MUSCL scheme is used to interpolate conservative variables at higher-order. A central difference method is used to discretize viscous term. Three-step and third-order strong-stability-preserving Runge-Kutta method (SSPRK) is used to time integration. A detailed chemical reaction system developed by Hong et al.^[10] is applied to oxy-hydrogen chemistry.

The schematic diagram of shock tube used for the present analysis is shown in Fig.1. The computational region is $300\text{ mm} \times 15.875\text{ mm}$ and the upper region is surface symmetrical boundary, right and bottom boundary are adiabatic wall, left boundary is out-flowing. Hence the total analytical region is two-dimensional shock tube with 31.75 mm in width. This width corresponds to the one of 1.25 inch which Myer and Oppenheim^[6] used for their H_2/O_2 auto-ignition experiment. The grid system is as follows; the right wall and bottom wall has concentrated grid system, the number of grid is 3000×301 points, the minimum grid size for x -direction and y -direction is 15.0 and $9.0\text{ }\mu\text{m}$, respectively.

As for the initial condition, the numerical shock tube has a high-pressure driver section and low-pressure driven section. The driven tube pressure, p_1 , and temperature, T_1 , are the same condition as Meyer and Oppenheim^[6] as 10 kPa and 296 K , respectively. The drive tube pressure, p_4 , and temperature, T_4 , are $100p_1$ and $1.25T_1$, respectively.

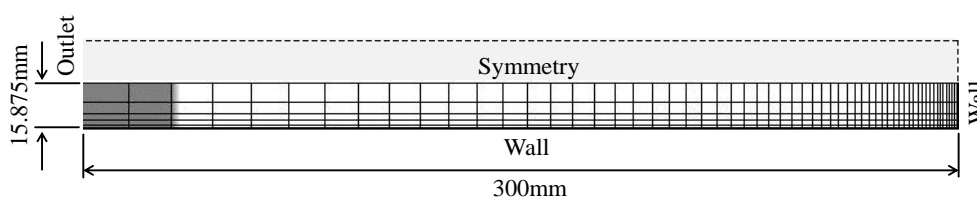


Fig. 1. Schematic diagram of shock tube system used in the present numerical analysis

3 Results and Discussions

3.1. Mild Ignition

At $p_4/p_1 = 200$ and $T_4/T_1 = 2.25$, mild ignition is observed near the right end wall of the shock tube shown in Fig.1. Figure 2 shows time histories of density gradient, temperature and vorticity distributions, where t is the time from shock wave reflection in the end wall and x is the distance from end wall. Hence the time is negative when shock wave moves from left to right as incident shock wave and it is positive when shock wave moves from right to left as reflected shock wave. At $t = 11.7\text{ }\mu\text{s}$ in Fig. 2(1), the incident shock wave has a one-dimensional structure with a very thin boundary layer. A

reaction shock does not appear yet behind the reflected shock wave in the mild ignition case, which is seen in the strong ignition case Meyer and Oppenheim(6) presented experimentally, because the induction time is longer in mild ignition than strong ignition. A lambda shock wave appears just after the incident shock wave reflects at the right tube end and its triple point moves upwards as the reflected shock wave propagates in the left direction (Fig.2(2)-(7)). At $t=40.8 \mu\text{s}$ (Fig.2-(7)), a flame kernel appears just behind the lambda shock wave near the wall to become mild ignition. In the present numerical case a contact surface comes to the lambda shock wave at this time.

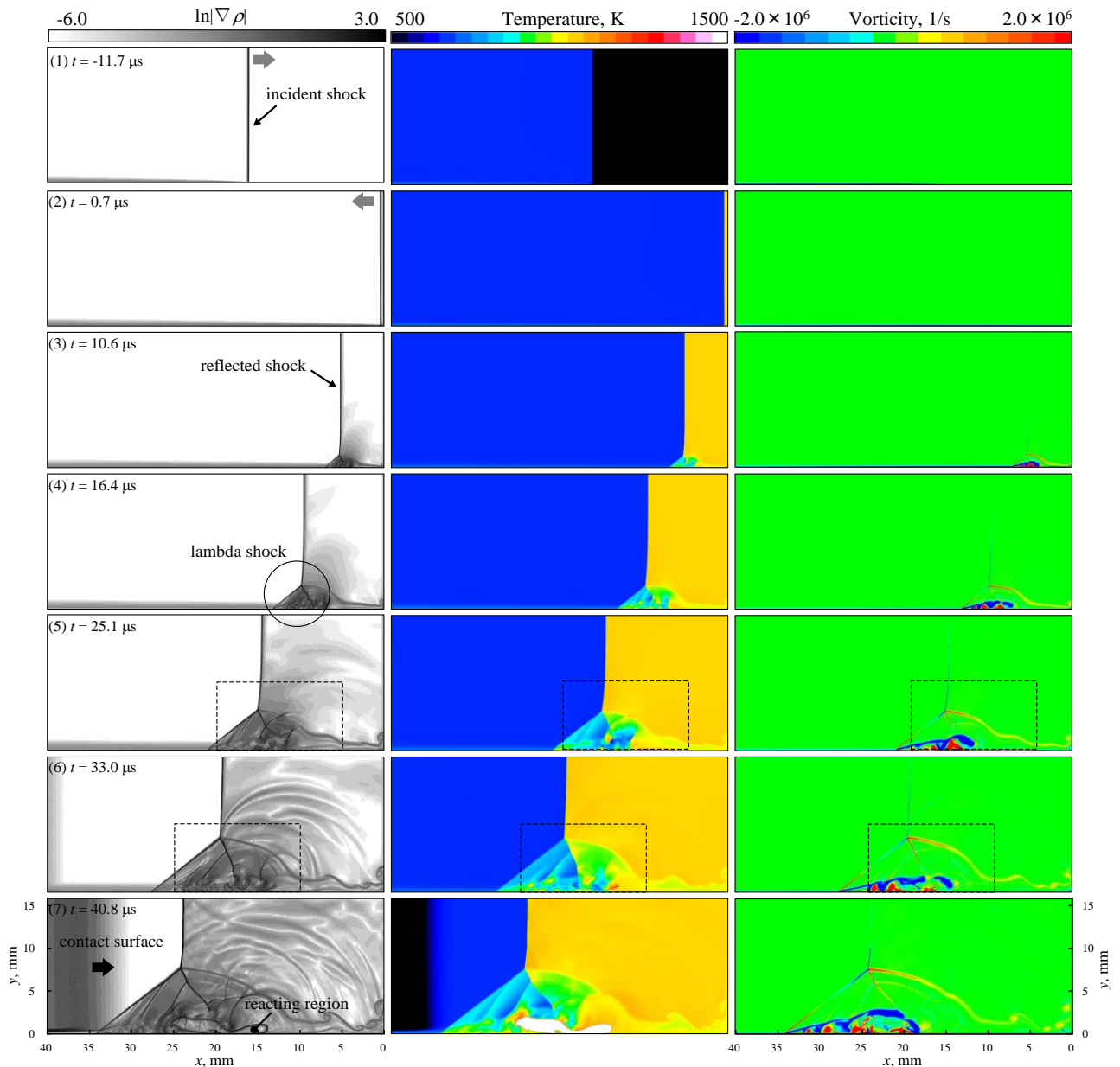


Fig. 2. The time histories of density gradient, temperature and vorticity distributions. The time when incident shock wave reaches the end wall is equal to zero.

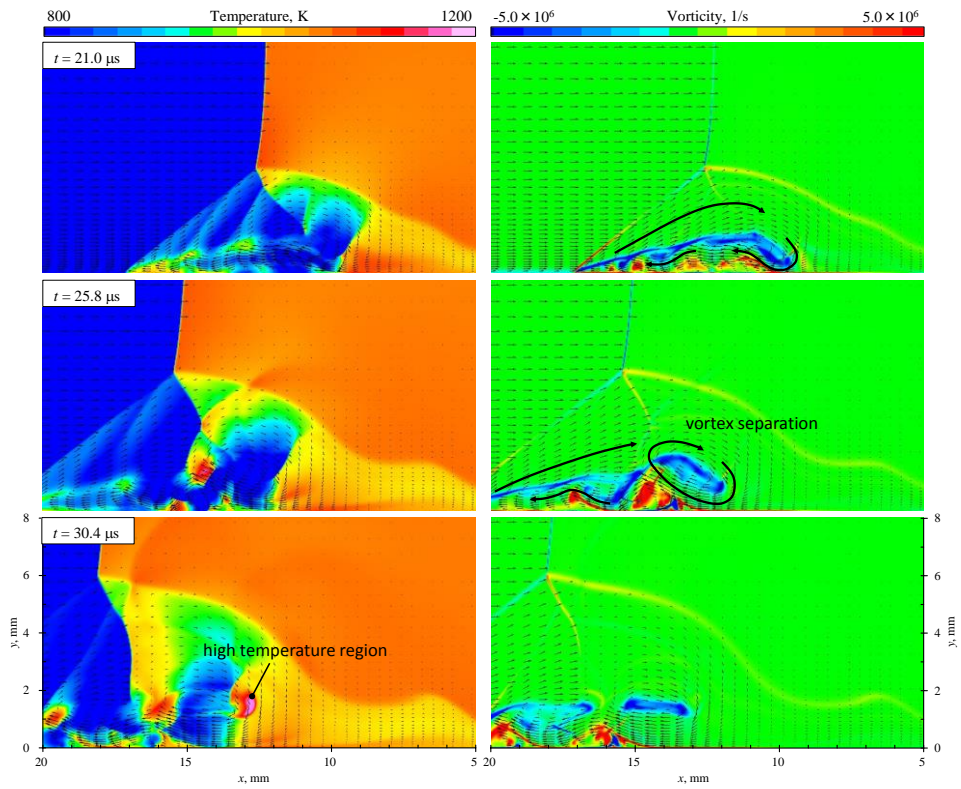


Fig. 3. The left figure is the spontaneous distributions of density and velocity vector in Fig.2-(5) at $t=25.1\mu s$.The right figure is the scketch of the left one.

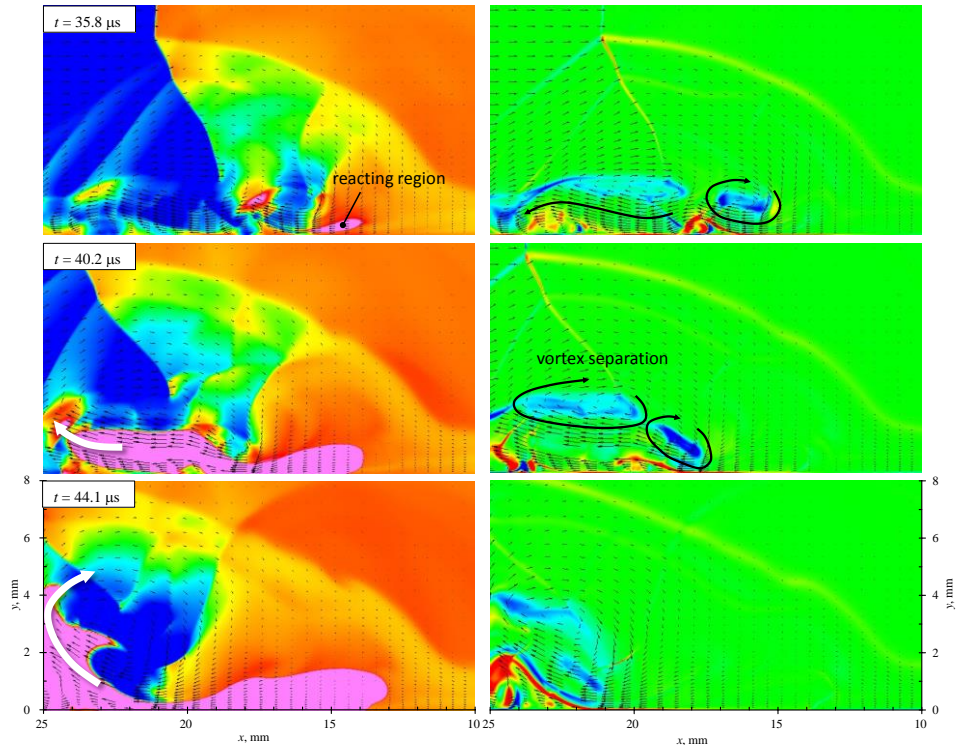


Fig. 4. The left figure is the spontaneous distributions of density and velocity vector in Fig.2-(6) at $t=33.0\mu s$.The right figure is the scketch of the left one.

Figs.3 and 4 show enlarged figures of the broken line region in Fig.2. Figure 3 shows the region where $5.0 \text{ mm} \leq x \leq 20.0 \text{ mm}$ and $0.0 \text{ mm} \leq y \leq 8.0 \text{ mm}$ and Fig.4 shows the region where $10.0 \text{ mm} \leq x \leq 25.0 \text{ mm}$ and $0.0 \text{ mm} \leq y \leq 8.0 \text{ mm}$. Both figures have logarithmic scale of temperature (left), vorticity (right) profiles, and velocity vectors (arrow). From the figures it is confirmed that a complicated lambda shock wave configuration appears by an interaction between viscous boundary layer and reflected shock wave. In the region behind the oblique shock wave at $t = 21.0 \mu\text{s}$, the clockwise vortex (blue region) and counter-clockwise (red region) appears alternately shown in vorticity distribution, but the largest vortex (pointed by arrow) governs the vertical flow. At $t = 21.0 \mu\text{s}$ the vortex detaches from the boundary layer and the section where the flow moves to the wall has high temperature. At the time $t = 35.8 \mu\text{s}$ the flow along the detached vortex is compressed near the wall to start reacting due to high temperature and pressure. The reacted gas propagates to the oblique shock wave along the flow and is rolled up near the oblique shock wave. The mild ignition may occur by an interaction between reflected shock wave and boundary layer after the process described above.

Several weak compression waves propagate upwards probably because of thermal expansion. Such compression waves are observed numerical analysis by Damezo et al.^[11] and experiments^[12]. Since the experiments by Yamashita et al.^[9] show an autoignition occurs at the location further away from the wall than that the triple point of lambda shock wave, hence not all the mild ignition occur from the interaction between reflected shock wave and boundary layer.

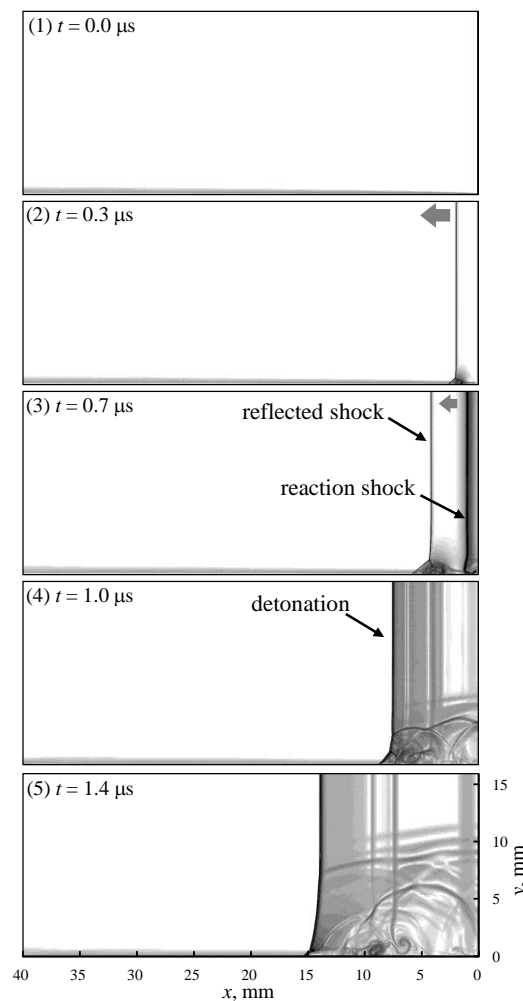


Fig. 5. Time histories of density gradient distribution of strong ignition case, where t is the time from shock wave reflection in the end-wall and x is the distance from end-wall.

3.2. Strong Ignition

Figure 5 shows density gradient profiles of strong ignition case near the end wall at $p_4/p_1=300$ and $T_4/T_1=2.50$. At $t = 0.3 \mu\text{s}$ reflected shock wave has a similar configuration (Fig.5(2)) to that of mild ignition case (Fig.2(2)). However at $t = 0.7 \mu\text{s}$ a reaction shock wave, which covers the whole width of the tube, appears and becomes detonation at $t = 1.0 \mu\text{s}$ (Fig.5(4)). This type of ignition process agree well with the process of strong ignition Meyer and Oppenheim(6) presented.

4 Conclusions

This study performed two-dimensional numerical analysis on reflected shock tube to find out a auto-ignition process in H₂/O₂ mixture behind reflected shock waves. The results reproduced mild and strong ignition behind reflected shock wave and especially the detailed process of mild ignition which has not been shown well in the past research. By the interaction between viscous boundary layer and reflected shock wave, the reflected shock wave has a lambda shock configuration. The flow behind lambda shock wave becomes complex vortices structure, then reactive gas mixture flowing along the detached vortices becomes under high temperature and pressure by compressed at the tube side walls. The chemical reaction starts at the location which reaches auto-ignition temperature to create flame kernels. The above story is appropriate in the process that flame kernel appears at the location between the triple point of lambda shock wave and tube wall, but is not insufficient in the process that flame kernel appears near the tube center which is above the triple point of lambda shock wave.

This paper presents the case of adiabatic wall condition, but the case of isothermal condition provides quite different physics from the present case. The future work will be performed the auto-ignition behind reflected shock wave under isothermal wall condition to compare with the adiabatic case.

References

- [1] Gilbert, R.B. and Strehlow, R.A., Theory of Detonation Initiation behind Reflected Shock Waves, AIAA J., 2: 783-784 (1966)
- [2] Strehlow, R.A. and Cohen, Limitations of the Reflected Shock Technique for Studying Fast Chemical Reactions and Its Application to the Observation of Relaxation in Nitrogen and Oxygen, A., J. Chem. Phys., 30: 257-265 (1959)
- [3] Saytzev, S.G. and Soloukhin, R.I., Study of Combustion of an Adiabatically-Heated Gas Mixture, 8th Symp. (Int.) Combust., 8: 344-347 (1962)
- [4] Voevodsky, V.V. and Soloukhin, R.I., On the Mechanism and Explosion Limits of Hydrogen-Oxygen Chain Self-Ignition in Shock Waves, 10th Symp. (Int.) Combust., 10: 279-289 (1965)
- [5] Soloukhin, R.I., Shock Waves and Detonations in Gases, Mono Book Corp.: 89-101 (1966)
- [6] Meyer, J.W. and Oppenheim, A.K., On the Shock-Induced Ignition of Explosive Gases, 13th Symp. (Int.) Combust., 13: 1153-1164 (1971)
- [7] Takano, Simulations of Bifurcation Processes of Reflected-Shock Waves in Ionizing Argon in a Shock Tube, Comput. Fluid, 19: 387-392 (1991)
- [8] Benkiewicz, K. and Hayashi, A.K., Aluminum Dust Ignition behind Reflected Shock Wave: Two-Dimensional Simulations, Fluid Dynamics Research, 30: 269-292 (2002)
- [9] Yamashita, H., Kasahara, J., Sugiyama, Y. and Matsuo, A., Visualization Study of Ignition Modes behind Bifurcated-Reflected Shock Waves, Combust. Flame, 159: 2954-2966 (2012)
- [10] Hong, Z., Davidson, D.F. and Hanson, R.K., An improved H₂/O₂ mechanism based on recent shock tube/laser absorption measurements, Combust. Flame, 159: 633-644 (2011)
- [11] Damazo, J., Ziegler, J., Karnesky, J. and Shepherd, J.E., Investigating Shock Wave-Boundary Layer Interaction Caused By Reflecting Detonations, 8th ISHPMIE paper, No.ISH-117 (2010)